Solubilization and characterization of extracellular proteins from anammox granular sludge

Boleij, Marissa; Seviour, Thomas; Wong, Lan Li; van Loosdrecht, Mark C.M.; Lin, Yuemei

DOI
10.1016/j.watres.2019.114952

Publication date
2019

Document Version
Final published version

Published in
Water Research

Water Research 164 (2019) 114952

Contents lists available at ScienceDirect

Water Research

journal homepage: www.elsevier.com/locate/watres

Solubilization and characterization of extracellular proteins from anammox granular sludge

Marissa Boleij [a], Thomas Seviour [b], Lan Li Wong [b], Mark C.M. van Loosdrecht [a], Yuemei Lin [a, *]

[a] Department of Biotechnology, Delft University of Technology, van der Maasweg 9, 2629, HZ, Delft, the Netherlands
[b] Singapore Centre for Environmental Life Sciences Engineering, Nanyang Technological University, 637551, Singapore

ARTICLE INFO

Article history:
Received 27 April 2019
Received in revised form
18 July 2019
Accepted 3 August 2019
Available online 4 August 2019

Keywords:
Anammox granular sludge
EPS
Ionic liquids
Alkaline extraction
Extracellular protein
β-sheet

ABSTRACT

Elucidating the extracellular polymeric substances (EPS) of anammox granular sludge is important for stable nitrogen removal processes in wastewater treatment. However, due to a lack of standardized methods for extraction and characterization, the composition of anammox granule EPS remains mostly unknown. In this study, alkaline (NaOH) and ionic liquid (IL) extractions were compared in terms of the proteins they extracted from different "*Candidatus* Brocadia" cultures. We aimed to identify structural proteins and evaluated to which extend these extraction methods bias the outcome of EPS characterization. Extraction was focussed on solubilization of the EPS matrix, and the NaOH and IL extraction recovered on average 20% and 26% of the VSS, respectively. Using two extraction methods targeting different intermolecular interactions increased the possibility of identifying structural extracellular proteins. Of the extracted proteins, ~40% were common between the extraction methods. The high number of common abundant proteins between the extraction methods, illustrated how extraction biases can be reduced when solubility of the granular sludge is enhanced. Physicochemical analyses of the granules indicated that extracellular structural matrix proteins likely have β-sheet dominated secondary structures. These β-sheet structures were measured in EPS extracted with both methods. The high number of uncharacterized proteins and possible moonlighting proteins confounded identifying structural (i.e. β-sheet dominant) proteins. Nonetheless, new candidates for structural matrix proteins are described. Further current bottlenecks in assigning specific proteins to key extracellular functions in anammox granular sludge are discussed.

1. Introduction

Anaerobic ammonium oxidation (anammox), a process involving the oxidation of ammonium to dinitrogen gas with nitrite as electron acceptor, is significant across many biogeochemical landscapes (De Brabandere et al., 2014; Kalvelage et al., 2013; Yang et al., 2015). The means to transform ammonium to nitrogen gas without oxygen also makes it a very attractive nitrogen removal process in wastewater treatment, where aeration is a major operating cost for complete nitrification. Since its discovery almost thirty years ago (Mulder, 1989), more than 100 full-scale applications have been commissioned in which anammox is coupled with partial nitritation (Lackner et al., 2014). This includes a wide spectrum of wastewaters that can be treated by anammox, from digester effluents (van der Star et al., 2007), black water from source separated sanitation (Vlaeminck et al., 2009), to various industrial wastewaters with low C/N ratio (Lackner et al., 2014). The configuration of the process ranges from two-stage to single-stage applying to either mainstream or side stream wastewater treatment plants. Currently there is a strong emphasis on developing anammox technology for mainstream municipal wastewater treatment (Agrawal et al., 2018; Cao et al., 2017; Hoekstra et al., 2018).

Anammox processes rely on the immobilisation of anammox bacteria as granules or biofilms, in order to reach sufficient biomass retention (Abma et al., 2007). Biofilm formation is facilitated by the production of extracellular polymeric substances (EPS) (Flemming, 2011). EPS are reported to consist of polysaccharides, proteins, DNA, and other polymers. The tendency of their EPS to mediate the

* Corresponding author.
E-mail address: Yuemei.Lin@tudelft.nl (Y. Lin).

https://doi.org/10.1016/j.watres.2019.114952

formation of dense anammox biofilms is an important aspect of stable anammox reactor operation. When the EPS are not sufficiently stabilised, this can impair the anammox process stability (de Graaff et al., 2011). On the other hand, EPS production can hamper the characterization of anammox cell biology (Cirpus et al., 2006). Hence, there are both cases in which EPS production is desirable and in which it is not. In any case it is a process with many unknowns, and therefore difficult to measure or control. To improve on that, it is important to first understand the composition of the EPS matrix.

In recent years, much information has been obtained regarding population, cell structure and compartmentalization (e.g. anammoxosomes) (Van Teeseling et al., 2013), and kinetics (Lotti et al., 2014). For example, five different genera have been identified that are capable of performing anammox (Peeters and van Niftrik, 2019). Nonetheless, despite their importance and ubiquity, the EPS are perhaps the least understood aspect of anammox communities. This is largely because EPS are difficult to analyse due to the fact that they are poorly soluble and compositionally heterogeneous (Seviour et al., 2019).

One major challenge, or objective in EPS characterization, is how to link EPS composition with function. Thus, instead of focussing on the amount of EPS (e.g. proteins and polysaccharides) that can be recovered, the composition should be identified to resolve the exact nature (Boleij et al., 2018; Felz et al., 2019; Seviour et al., 2019). In previous work it was shown that proteins form the dominant fraction in the EPS (Boleij et al., 2018; Chen et al., 2019), and anammox EPS contains a relatively high amount of β-sheets (Hou et al., 2015). β-Sheets have the potential to self-assemble into various conformations that can have structural functions in the matrix (Perras et al., 2015) (e.g. as fibers, like silk (Pena-Francesch and Demirel, 2019) or amyloid-like (Lotti et al., 2019)). Hence, β-sheet rich proteins potentially have a structural function in the EPS matrix.

The prerequisite step for recovery and identification of the structural polymers, is to solubilize the EPS. Because different biofilms have different EPS, various biofilms need a different treatment to be solubilized. For example, some aerobic granules were effectively solubilized with alkaline conditions (Felz et al., 2016), while this treatment did not work for aerobic granules enriched with *Defluviicoccus* (Pronk et al., 2017) and aerobic granules enriched with ammonia-oxidizing bacteria (Lin et al., 2018). Instead, they were solubilized with acidic conditions and SDS treatment, respectively.

Studies involving EPS extraction from anammox granular sludge, in general don't report the solubilization of the EPS matrix. Two previously proposed extraction methods that were able to solubilize and recover EPS of anammox granular sludge, are the alkaline (NaOH) extraction (Boleij et al., 2018) and ionic liquid (IL) extraction (Wong et al., 2019). However, they were never directly compared. Since there are no standardized extraction and characterization methods, it is currently unknown if these two extraction methods lead to comparable extracted EPS or not.

Here we evaluated two different extraction methods (NaOH and IL) and analysed the extracted EPS from anammox granular sludge from various reactors, focussing on proteins. The molecular weight distribution and the functional groups of the recovered EPS were investigated, as well as the secondary structure of the extracted proteins. Mass spectrometry (MS) was applied for identification of extracted proteins. The recovered polymers were characterized in order to evaluate the influence of different extraction methods, and better understand the underlying extraction mechanisms. In addition, by combining information of the characterization of EPS extracted with both methods, we aimed for identification of the structural components.

2. Materials and methods

2.1. Sampling and characterization of anammox granular sludge

Anammox granular sludge samples were collected from three full-scale plants in the Netherlands (NlAmx1, NlAmx2 and NlAmx3) as well as from a lab-scale reactor in Singapore (SgAmx). The characteristics of all reactors are shown in Table 1. A clone library analysis was performed to identify the dominant anammox species in the granules. This was complemented by Fluorescent In Situ Hybridization (FISH), which was performed as described by Johnson et al. (2009) (see supplemental materials for details about clone library analysis and FISH).

Anammox granules were visualized with an optical microscope, scanning electron microscope and transmission electron microscope. The granular sludge sample with the highest inorganic content (NlAmx1) was analysed by micro-computed tomography (Micro-CT). Micro-CT was performed as described by Lin et al. (2013), using a MCT-12505MF (Hitachi Medical, Kashiwa, Japan).

Thioflavin T staining was performed to indicate β-sheet rich structures in the granule. 0.5% (w/v) Thioflavin T (THT) (Sigma Aldrich) was prepared in 0.1N HCl and filtered. Cryosectioned anammox granules (Leica Cyrostats CM1950) on glass slide (5 μm) was stained with THT working solution for 15 min and the slide was rinsed two times with PBS and imaged on Leica SPP8WLL confocal microscope with a 40× objective.

2.2. EPS extraction by ionic liquid treatment

Prior to extraction, granules were washed with MilliQ water and lyophilized. The EPS extraction process was performed as follows: Ionic liquid (IL) 1-ethyl-3-methyl imidazolium acetate (EMIA) was mixed with dimethylacetamide (DMAc) to a volumetric ratio of 40:60 as described in Seviour et al. (2015). Freeze-dried anammox granules were directly added to 15 mL 40% v/v EMIA mixture to a concentration of 30 mg/mL in a Falcon tube. The tube was incubated in a 55 °C water bath for 16 h. Soluble and semi-soluble fractions were captured by precipitation with ethanol (70% v/v), separated by centrifugation, cleaned by dialysis and lyophilized for further analysis.

2.3. EPS extraction by alkaline treatment

The alkaline (NaOH) extraction was performed as described in Boleij et al. (2018). Freeze-dried anammox granules were added to 0.1 M NaOH to a concentration of 50 mg/ml. The mixture was incubated for 5 h while being stirred with a magnetic stirrer at 400 rpm. After centrifugation at 4000*g* for 20 min at 4 °C, the pellet was discarded. Polymers in the supernatant were precipitated out by decreasing the pH to 5. For 40 ml solution, ~2.5 ml HCl (1M) was used to obtain pH 5. The precipitated polymers were collected by centrifugation at 4000*g* for 20 min at 4 °C. Subsequently the extracted EPS were dialyzed and lyophilized.

2.4. Live/dead staining

IL and NaOH treated anammox granules were examined by live/dead staining. Briefly, anammox granules (treated and untreated), were washed two times with double distilled water and freeze-dried. Subsequently they were stained with BacLight Live/Dead viability stain (Thermo Fisher Scientific). Live/dead stain was prepared by adding 6 μL of 1:1 SYTO 9 (3.34 mM in DMSO) and propidium iodide (20 mM in DMSO) mixture to 1 mL of double distilled water. After staining for 15 min, the granules were washed two times with double distilled water for 5 min, smeared on glass slides

Table 1
Characteristics of the different reactors and anammox granular sludge.

Sample	NlAmx1	NlAmx2	NlAmx3	SgAmx
Reactor	full-scale the Netherlands	full-scale the Netherlands	full-scale the Netherlands	lab-scale Singapore
Wastewater	municipal	industrial[a]/municipal	industrial[b]	synthetic
System	anammox	nitratation/anammox	nitritation/anammox	anammox
Feed NH_4^+ (mg N L^{-1})	500 − 700	300 − 400	1000 − 2000	300 ± 20
Feed NO_3^- (mg N L^{-1})	500 − 700	none	none	360 ± 20
Volume (m^3)	70	600	3000	0.004
DO (mg O_2 L^{-1})	0	0.5 − 2	0.5 − 1.5	<0.01
pH	7.0 − 7.5	7.5 − 8.0	7.0 − 7.5	7.0 − 7.5
VSS in granules (%)	71	88	87	88

[a] Potato plant.
[b] Rendering plant.

and imaged on confocal microscope (Leica SP8WLL and Zeiss LSM 780 with a 63× objective).

2.5. Fourier-transform infrared (FTIR) spectroscopy and excitation-emission matrix (EEM) fluorescence spectroscopy

The Fourier-transform infrared (FTIR) spectra of the extracted EPS were recorded on a FTIR Spectrometer (PerkinElmer, Shelton, USA) at room temperature, with the wavenumber range from 550 cm^{-1} to 4000 cm^{-1}.

3D fluorescent spectroscopy of extracted EPS solutions (25 mg/L, pH 11) was performed using a FluoroMax-3 spectrofluorometer (HORIBA Jobin Yvon, Edison, NJ, U.S.A.). EEM spectra were scanned with excitation wavelengths from 220 to 450 nm (2 nm increment) and emission wavelengths from 270 to 500 nm (4 nm increment). Graphs were generated using MATLAB.

2.6. SDS-PAGE (sodium dodecyl sulfate − polyacrylamide gel electrophoresis)

The extracted EPS were analysed by SDS-PAGE, as described in Boleij et al. (2018). SDS-PAGE was performed using NuPage® Novex 4–12% Bis-Tris gels (Invitrogen). EPS samples were prepared in NuPAGE LDS-buffer and DTT (dithiothreitol) was added to a final concentration of 10 mM. The proteins were denatured by incubation at 70 °C for 10 min. Subsequently, 10 µl sample was loaded per well. The Thermo Scientific Spectra Multicolor Broad Range Protein Ladder was used as molecular weight marker. The gel electrophoresis was performed at 200 V for 35 min. The gels were stained by three different stains afterwards.

For visualization of proteins, the Colloidal Blue staining kit (Invitrogen) was used according to manufacturer's instructions. For visualization of glycoproteins, the Thermo Scientific Pierce Glycoprotein Staining Kit was used, which is based on the periodic acid-Schiff (PAS) method and is specific for glycans bearing vicinal hydroxyl groups. For staining of acidic glycoconjugates, Alcian Blue 8GX (Fluka, Sigma Aldrich) was used. Alcian Blue is a cationic dye. It was used with pH 2.5 to stain dissociated (ionic) acidic groups. An adapted protocol of Møller and Poulsen (2009) was used. After electrophoresis, the gels were extensively washed in solution I (25% (v/v) ethanol and 10% (v/v) acetic acid) for 2.5 h while refreshing the solution 4 times. Subsequently, the gel was stained in 0.125% (w/v) Alcian Blue in solution I for 30 min and washed in solution I overnight.

2.7. Mass spectrometry (MS) analysis

The samples, containing 100 µg of proteins, were polymerized in a 4% SDS gel and fixed with 50% methanol and 12% acetic acid, for 30 min in room temperature. The gel was cut into small pieces (1 mm^3), the pieces were washed three times with 50 mM TEAB/50% (v/v) acetonitrile (ACN) and dehydrated using 100% ACN. Samples were reduced with 5 mM TCEP at 57 °C for 60 min, followed by alkylation with 10 mM MMTS for 60 min at room temperature with occasional vortexing. Following reduction and alkylation, the gel pieces were washed with 500 µl of 50 mM TEAB. They were dehydrated with 500 µl of ACN and 500 µl of 50 mM TEAB added for re-swelling. A final dehydration step was performed using 100 µl of ACN. 1 µg of trypsin per 20 µg of proteins was added and trypsinization performed at 37 °C for 16 h. The digested peptides were extracted sequentially with 200 µl each of 50 mM TEAB, 5% formic acid (FA) in 50% ACN and then 100% ACN. The solutions were added, allowed to stand for 5–10 min and centrifuged at 6000 rpm. The supernatant with the digested peptides were collected. Elutes were then desalted in a Sep-Pak C18 cartridge (Waters, Milford, MA), dried and then reconstituted in 20 µl of 2% ACN and 0.05% FA in water. An Eksigent nanoLC Ultra and ChiPLC-nanoflex (Eksigent, Dublin, CA, USA) column was used in Trap Elute configuration to separate the peptides. Desalting was with a Sep-Pak tC 18 µ Elution Plate (Waters, Miltford, MA, USA), followed by reconstitution in 20 µl of 2% ACN and 0.05% FA in water. 5 µl of the samples were loaded on a 200 µm × 0.5 mm trap column and eluted through an analytical 75 µm × 150 mm column made of ChromXP C18-CL, 3 µm (Eksigent, Germany). Peptides were separated by a gradient formed by 2% ACN, 0.1% FA and 98% ACN, 0.1% FA. A TripleTOF 5600 system (AB SCIEX, Foster City, CA, USA) in Information Dependent Mode was used for MS analysis. MS spectra were acquired across the mass range of 400–1250 m/z in high resolution mode (>30000) using 250 ms accumulation time per spectrum. Tandem mass spectra were recorded in high sensitivity mode (resolution >15000) with rolling collision energy on adjustment. Survey- IDA Experiment, with charge state 2 to 4 was selected. Peptide identification was carried on the ProteinPilot 5.0 software Revision 4769 (AB SCIEX) using the Paragon database search algorithm (5.0.0.0.4767) for peptide identification and the integrated false discovery rate (FDR) analysis function. The data were searched against a "*Ca.* Brocadia" database (total 33264 sequences). These protein data were searched against a protein reference database obtained from analysis of translated predicted genes from metagenome assemblies of the sampled reactor communities combined with protein sequence from five extant draft AnAOB genomes (Liu et al., 2018).

2.8. Analysis of abundant protein sequences

To estimate the protein abundance in the samples, Exponentially Modified Protein Abundance Index (emPAI) analysis was performed according to Li et al. (2016). The sequences of the

abundant proteins, obtained with the emPAI analysis, were subjected to the PredictProtein tool to predict structural and functional features (Yachdav et al., 2014), and the ProtParam tool from ExPaSy to predict physical and chemical parameters (Gasteiger et al., 2005).

3. Results

3.1. Characterization of the anammox granular sludge

Granules from three full-scale (municipal and industrial) and one laboratory-scale anammox reactor (see Table 1) were collected in order to extract their EPS and resolve the composition. The phylogenetic tree in Fig. 1 shows that the dominant anammox species in NlAmx1 and NlAmx3 cluster together, and in both instances are closely related to "*Candidatus (Ca.)* Brocadia sapporoensis" (previously "*Ca.* Brocadia sp. 40"). NlAmx2 and SgAmx cluster together and are closely related to "*Ca.* Brocadia sinica". A smaller part of SgAmx is closely related to "*Ca.* Brocadia caroliniensis". FISH indicated a high abundance of the anammox bacteria in the granules (see Supplemental Figs. S1 and S2).

The volatile suspended solid (VSS) content of the granules ranged from 71 to 88% (Table 1). In Fig. 2B, the inorganic part appears bright and is not only present in the core of the granules, but also forms layers around the core. The inorganic fraction of NlAmx1 was previously determined to be hydroxyapatite (Lin et al., 2013). In between these hydroxyapatite layers the space is filled with the organic matrix, which appears as the grey part. The matrix of the granules has a heterogeneous structure, as was observed using electron microscopy: both regions with low and high cell densities were observed. In regions with low cell densities, both a compact matrix and a relatively open, fibrous structure can be seen (Fig. 2C and D). At the regions with high cell densities, the EPS appear in between the cells, which glue the cells tightly to each other (Fig. 2E and F). Thus, the challenge for the EPS characterization lies not only in the fact that the EPS matrix is difficult to solubilize, but also in the heterogeneous structure of the granules.

Thioflavin T (ThT) staining was applied to indicate β-sheets in the anammox granules. ThT becomes strongly fluorescent when it binds to β-sheet rich structures. The images in Fig. 3 show that ThT binds to the anammox granules enriched with "*Ca.* Brocadia sinica", which indicates that β-sheets are indeed a dominant secondary structure in the EPS. Since β-sheets are abundant, and also found before in anammox EPS (Lotti et al., 2019), for the EPS analysis in this study, β-sheet rich proteins will be taken into account as a candidate for structural extracellular proteins.

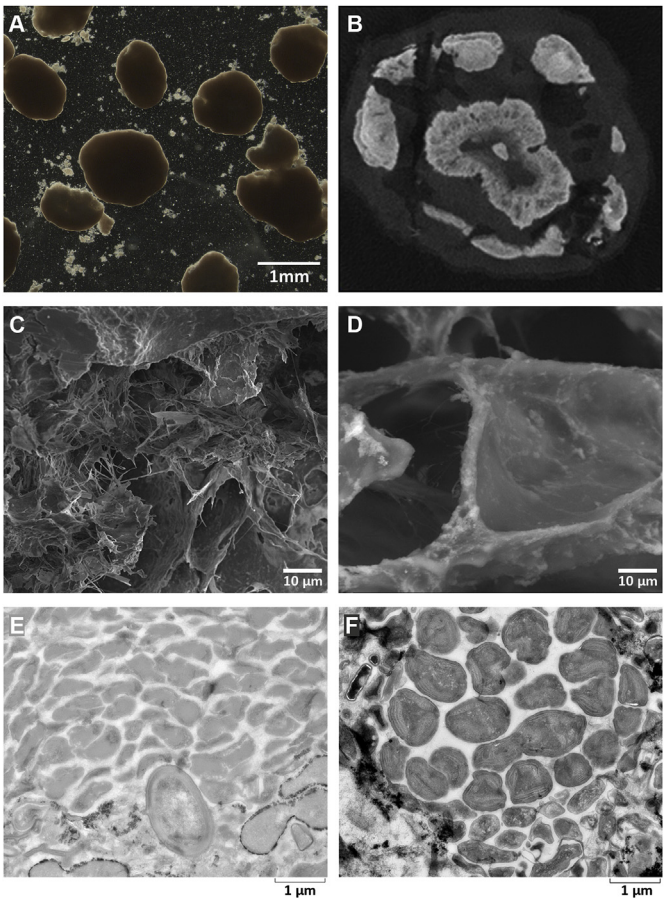

Fig. 2. Visualization of anammox granular sludge. A) Optical microscope image. B) micro-CT scan of one intact anammox granule. The bright part is the mineral hydroxyapatite, and the grey part is the organic matrix. C) and D) are scanning electron microscopy pictures of the inside of the granules where the structure of the matrix of granules enriched with "*Ca.* Brociadia sapporoensis" and "*Ca.* Brocadia sinica" respectively. E) and F) are transmission electron microscopy pictures of cells that are glued to each other by their EPS, in granules enriched with "*Ca.* Brocadia sapporoensis" and "*Ca.* Brocadia sinica" respectively.

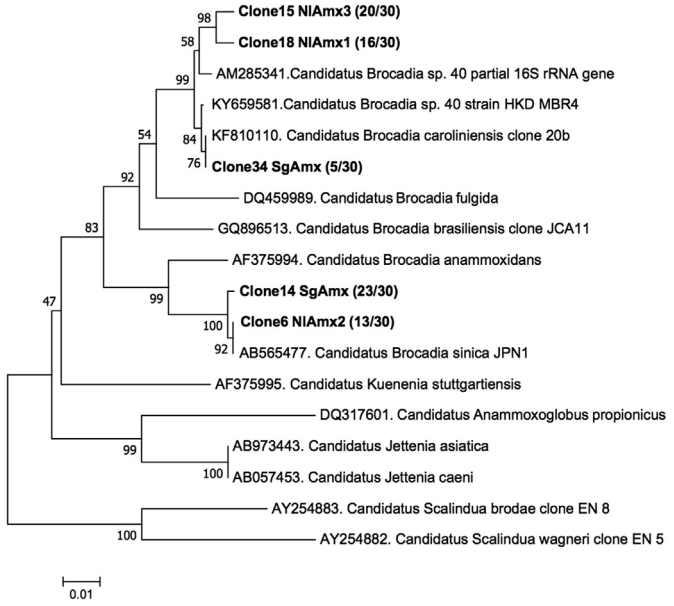

Fig. 1. Phylogenetic tree with the anammox bacteria of the different reactors, determined by a clone library analysis.

3.2. Solubilization of anammox granules by alkaline (NaOH) and ionic liquid (IL) treatments

The granular sludge from all four anammox reactors was subjected to alkaline (NaOH) and ionic liquid (IL) extractions. The extractions were performed according to the workflow scheme in Fig. 4. Following NaOH treatment, the granular shape was lost (Fig. 5A), indicating the dissolution of structural EPS. To precipitate the solubilized polymers, HCl was added dropwise until the pH was decreased to pH 5. This resulted in the formation of gel-like films, which could be recovered by centrifugation. After IL treatment there is a stratification of the granular matrix into a mineral part (lower layer), a gel layer (middle layer) and a soluble layer (upper layer) (Fig. 5A). The upper and the middle layers were recovered. The upper layer was soluble in water (IL-Sol) while the middle layer was insoluble in water (IL-Gel).

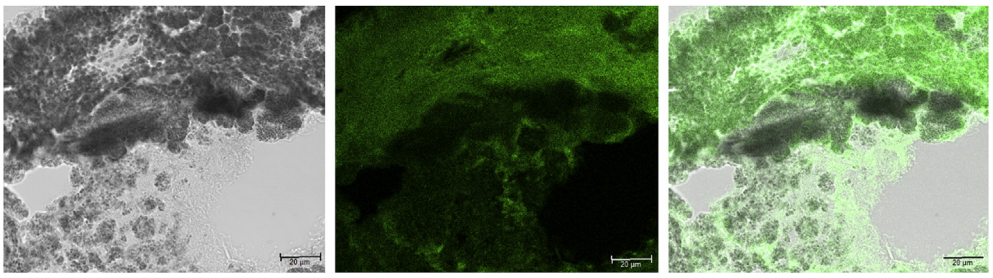

Fig. 3. Staining of the anammox granule enriched with "Ca. Brocadia sinica" with Thioflavin T (ThT). Microscopy image (left), fluorescent microscopy image after staining with ThT (middle) and overlay of both images (right). (Scale bar is 20 μm)

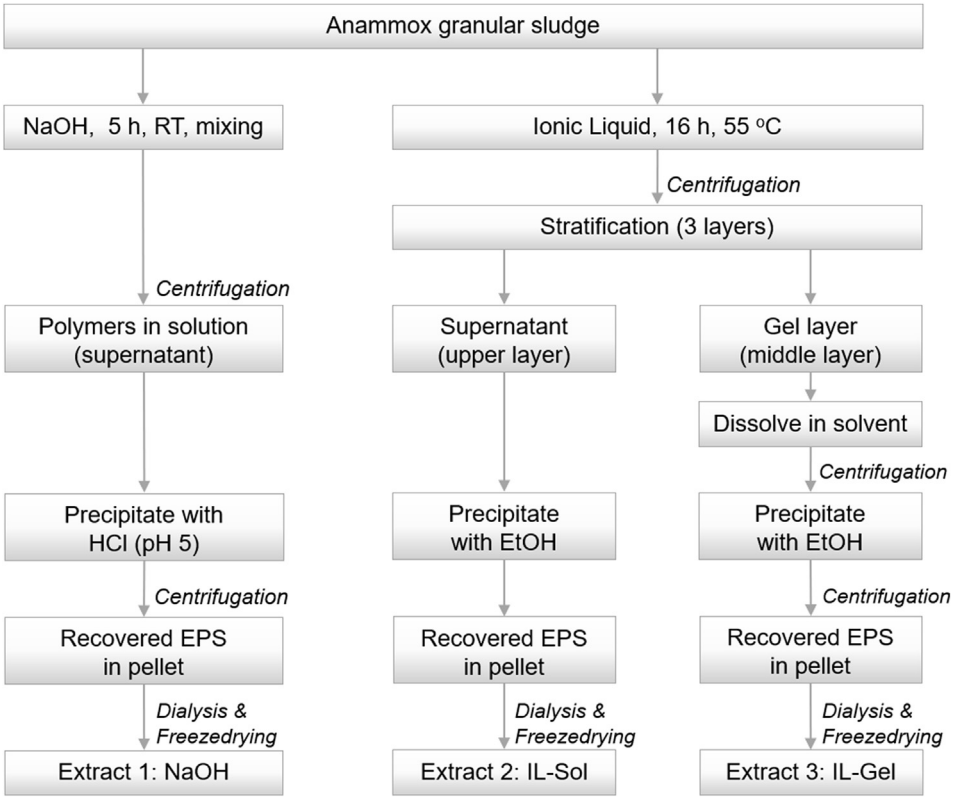

Fig. 4. Workflow of the 2 different extraction methods, leading to the 3 extracts; NaOH, IL-Sol, IL-Gel.

Using the NaOH extraction method, approximately 20% of the VSS is extracted, whereas with the IL extraction method up to 30% of the VSS is extracted (Fig. 5B). Both treatments caused disintegration of the granular shape. The VSS components that could not be solubilized stayed in the pellet together with the inorganic part of the granules. Compared to the NaOH and IL-Gel fractions, the IL-Sol fraction is only a minor fraction of the EPS. Interestingly, the dried IL-Sol fraction was a white powder while the NaOH and the IL-Gel fractions were both red.

Harsh extraction methods were used to solubilize the granular sludge, possibly leading to cell death. Live/dead staining of the treated anammox cells (Fig. 5C) shows that IL and NaOH treatments resulted in more staining of the biomass by propidium iodide (red) than the control, which indicates either greater cell permeability or DNA release due to lysis. However, even before extraction there is a significant amount of dead cells present in the granular sludge.

In summary, the results of the extractions showed that both extraction methods fulfil the first requirement of EPS extraction, namely the solubilization of the granular matrix. Because ionic liquid and NaOH treatments damage the cells, it can not be excluded that intracellular proteins are released and co-extracted. For convenience, we will refer to the total extracted material by 'extracted EPS'. The extracted EPS will be characterized with a focus on potential extracellular properties (e.g. high amount of beta-sheets as was found in the granular matrix), and assigning intra- and extracellular proteins using mass spectrometry. Hereby aiming at identification of extracellular proteins and additionally validating the recovery of extracellular polymers with these extraction methods.

3.3. β-sheets dominate the secondary structure of extracted proteins

FTIR was applied in order to analyse the protein secondary structure and to explore functional groups in the extracted EPS. The FTIR profiles of the EPS from the different reactors were comparable

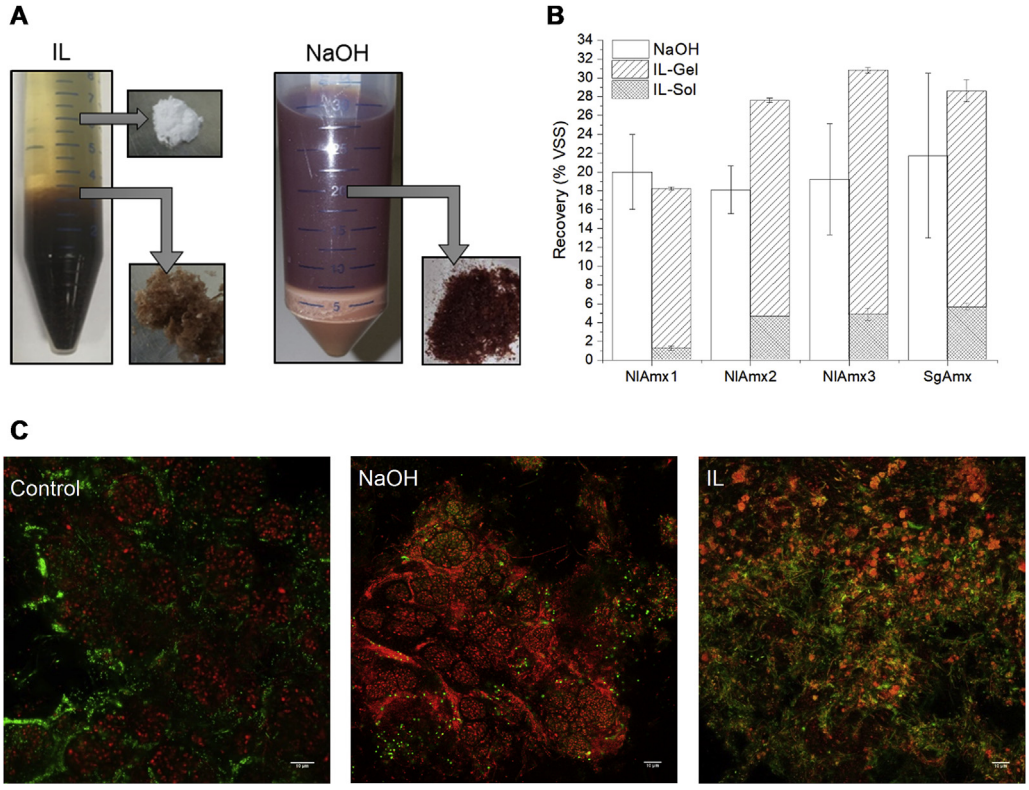

Fig. 5. EPS extractions by IL and NaOH treatment. A) Images of the solubilization of the granules in IL and NaOH, and the three recovered fractions B) Recovery yield of the NaOH and IL extraction on the different biomass samples. C) Live/dead staining before treatment (left), and after NaOH (middle) or IL treatment (right). Staining by propidium iodide (red) indicates dead cells and staining with SYTO (green) indicates living cells. (Scale bar is 10 μm). (For interpretation of the references to color in this figure legend, the reader is referred to the Web version of this article.)

(see Supplementary Fig. S3). Thus, based on the FTIR the functional groups of the different granular sludge samples look similar. In Fig. 6 the FTIR spectra of extracted EPS from "*Ca.* Brocadia sinica" (NlAmx2) are shown as an example for the comparison of the EPS extracts NaOH, IL-Gel and IL-Sol. The FTIR spectra of NaOH extracted EPS and IL-Gel EPS are similar: A narrow band with a relatively sharp peak at 3280 cm^{-1}, which is a typical peak of −NH group in proteins. A peak at 3050 cm^{-1}, indicating the presence of aromatic amino acids (tryptophan, tyrosine, and phenylalanine)

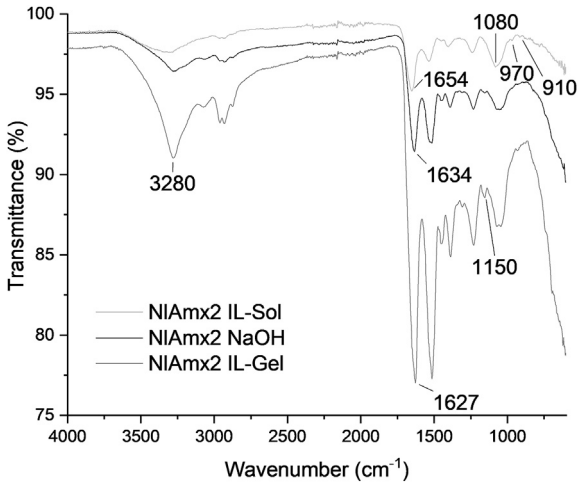

Fig. 6. FTIR spectra of 3 different fractions, extracted from NlAmx2 ("Ca. Brocadia sinica").

(Dian et al., 2002). The dominant protein secondary structure are β-sheets with the peak at 1635 cm^{-1} of NaOH extracted EPS and the peak at 1627 cm^{-1} of IL-Gel EPS (Barth, 2007). The peak at 1150 cm^{-1} implies there are C—O—C bonds due to the crosslinking of acidic sugars (e.g. sugars with —COOH group). A band at 1200-940 cm^{-1} with two peaks, one peak at 1080 cm^{-1} due to the presence of $-PO_4^{3-}$, and the other one at 1040 cm^{-1}, indicating carbohydrates.

In comparison, the spectrum of IL-Sol is different in the following peaks: a broad band at 3700—3100 cm^{-1} with peak at 3280 cm^{-1}, which is assigned to hydroxyl group (—OH); a peak at 1654 cm^{-1} indicating the dominant protein secondary structure is α-helix (Barth, 2007); a band at 1200-940 cm^{-1} with the peak at 1080 cm^{-1}, implying that there are carbohydrates and $-PO_4^{3-}$ groups, the strong signal of $-PO_4^{3-}$ covers the peak of carbohydrates. There are two extra peaks at 970 cm^{-1} and 910 cm^{-1} from $-PO_4^{3-}$ group, matching with the strong signal of phosphate. In addition, no peak at 3050 cm^{-1}, indicating there is little aromatic amino acids (tryptophan, tyrosine, and phenylalanine) (Dian et al., 2002); and no peak at 1150 cm^{-1} implying there is little C—O—C bond from the crosslinking of acidic sugars.

Thus, NaOH extracted EPS and IL-Gel EPS are dominated by proteins with β-sheet secondary structure, while proteins in the IL-Sol fraction is dominated with α-helix secondary structure, and phosphate groups (especially with hydroxyl groups, such as hydroxyapatite). The high amount of β-sheets are consistent with what was observed with the ThT staining.

In addition to the FTIR, EEM spectra of the three extracts were measured (Fig. 7 and Supplementary Fig. S4). While both NaOH and IL-Gel have a major peak at 275/340 (ex/em), the IL-Sol has a very

small signal at those wavelengths, and a major peak at 240/360 instead. The 275/340 nm peak is reported to represent aromatic amino acid tryptophan. The 240/360 peak is the same as the peak for the autofluorescence of hydroxyapatite (Ciobanu et al., 2012). The high amount of tryptophan is in accordance with the FTIR spectra, where the 3050 cm^{-1} peak showed phenolic amino acids. Tryptophan plays an important role in the formation of β-sheets. As β-sheet structures are dominant in the NaOH and IL-Gel samples, more tryptophan is present in these fractions than in the IL-Sol sample.

3.4. Protein profile of extracted EPS depends more on dominant population than extraction method

The protein profiles of the different extracts were compared by using SDS-PAGE analysis, in combination with different stains. Proteins, neutral glycans and acidic glycans, that were also indicated with FTIR, were stained with Coomassie Blue, Periodic acid Schiff (PAS) and Alcian Blue, respectively. In Fig. 8, pictures of SDS-PAGE gels with extracted EPS of NlAmx1 (representative for "*Ca.* Brocadia sapporoensis") and NlAmx2 (representative for "*Ca.* Brocadia sinica") are shown (see Supplementary Fig. S5 for all sludges). IL and NaOH methods both extracted glycoproteins, as indicated by the bands that stained positive for both Coomassie Blue and PAS stains. For NlAmx1 glycoproteins were observed at 80, 12 and 10 kDa, regardless of the extraction methods used. For NlAmx2, IL extracted EPS showed glycoprotein bands at 200, 150, 50 and 8 kDa. NaOH-extracted EPS also showed the 8 kDa band while the higher molecular weight glycoproteins appeared less resolved. Thus, the protein profile of the extracted EPS depended more on dominant population than on the extraction method.

In addition, the Alcian Blue staining, that is specific for glycoconjugates with an acidic character (carboxylated or sulfated), showed that the NaOH extraction recovered more acidic polymers than the IL-Gel, which is indicated by the 'smear' in the high molecular weight range (>235 kDa). This was the case for both NlAmx1 and NlAmx2. For the IL-Sol, a larger sample amount needed to be applied to visualize the bands, indicating a lower presence of proteins in this fraction.

3.5. In search of structural extracellular (glyco)proteins

To identify proteins with a potential function in the structural matrix, the extracted EPS from NlAmx1 ("*Ca.* Brocadia sapporoensis") and SgAmx ("*Ca.* Brocadia sinica") were analysed using mass spectrometry (MS). All fractions from the extractions were analysed to compare the results of the NaOH and IL methods. The obtained spectra were matched against a "*Candidatus* Brocadia" wide database. Of the detected proteins in the NaOH extracted EPS, 59% and 62% was also detected when EPS was extracted with the IL method, for NlAmx1 and SgAmx respectively. Of the total detected proteins 41.5% and 37.1% are overlapping for NlAmx1 and SgAmx respectively, as illustrated in Fig. 9. The amount of detected proteins in NaOH and IL extracted samples are comparable in the case of NlAmx1, while for SgAmx the amount of detected proteins was higher for the IL extracted EPS. Of the IL soluble proteins, 63% and 60% for NlAmx1 and SgAmx respectively are also detected in the IL gel proteins (Supplementary Fig. S6).

The emPAI method was applied to find the relative abundance of the proteins in the extracted EPS. A list with abundant proteins in the different fractions is shown in Table 2. Considering abundant proteins in the different extracts, similar predicted functions could be found. Various enzymes, proteases, superoxide dismutases, chaperones, a heme transporter and elongation factor Tu, and uncharacterized proteins were found. The emPAI analysis shows similar types of proteins that are abundant in both "*Ca.* Brocadia sapporoensis" and "*Ca.* Brocadia sinica" (Supplementary Tables S1–6).

The sequences of the abundant proteins were analysed with online tools (ExPaSy, ProtParam and PredictProtein) that predict various physical and chemical parameters like subcellular localization, secondary structure, grand average of hydropathicity (GRAVY), aliphatic index and instability index of the proteins. The proteins that were predicted to be extracellular proteins (including secreted and fimbrium proteins) all belong to the uncharacterized proteins, which means that the function is still unknown. Among the predicted secreted proteins, especially A0A1V6LWI7 was noticed for its secondary structure was predicted to contain no α-helix, but only β-sheet (42%) and loop structures (58%). This is similar as in the previously identified glycoprotein in "*Ca.* Brocadia sapporoensis", which was proposed to be a surface layer protein (Boleij et al., 2018), and which contains 47% β-sheet and 53% loop structures. Looking at the conserved domains present in the sequence of A0A1V6LWI7, it contains a WD40/YVTN repeat domain. Structurally, both the WD40 and the YVTN repeated motifs form a circularised beta-propeller structure, which consist of seven 4-stranded beta-sheets. Looking to the aligned PDB (protein database bank) homologs, the structure of the protein A0A1V6LWI7 is related to the structure of a hydrazine synthase (E-value: 9e-84) and of a surface layer protein of archaea bacteria (E-value: 7e-54)

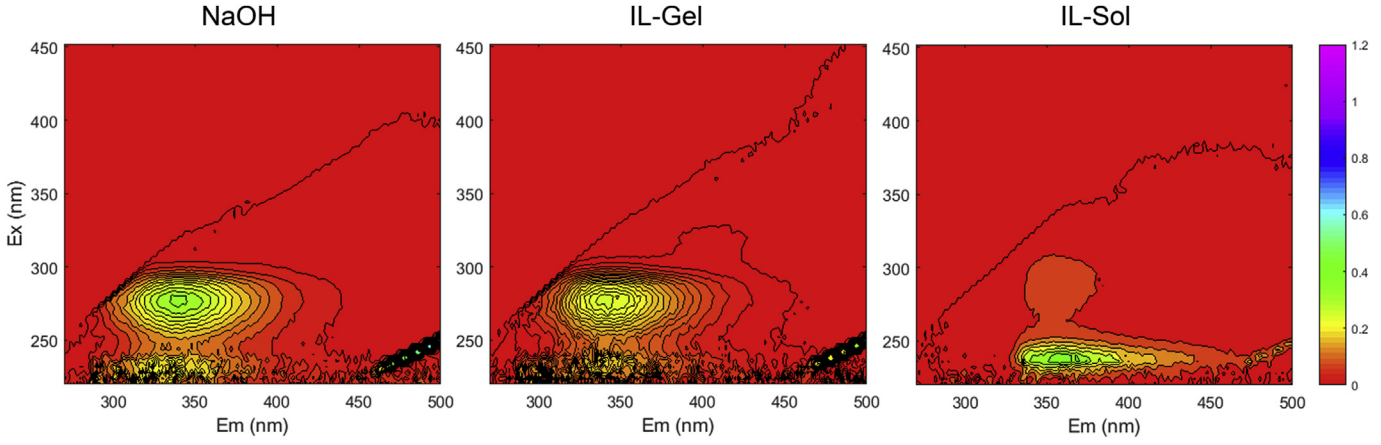

Fig. 7. Excitation Emission spectra of the different fractions (NlAmx 2, *Ca.* Brocadia sinica). The NaOH (left) and the IL-Gel (middle) fraction have a peak at 275/340 nm while the IL-Sol (right) fraction has the major peak at 240/360 nm.

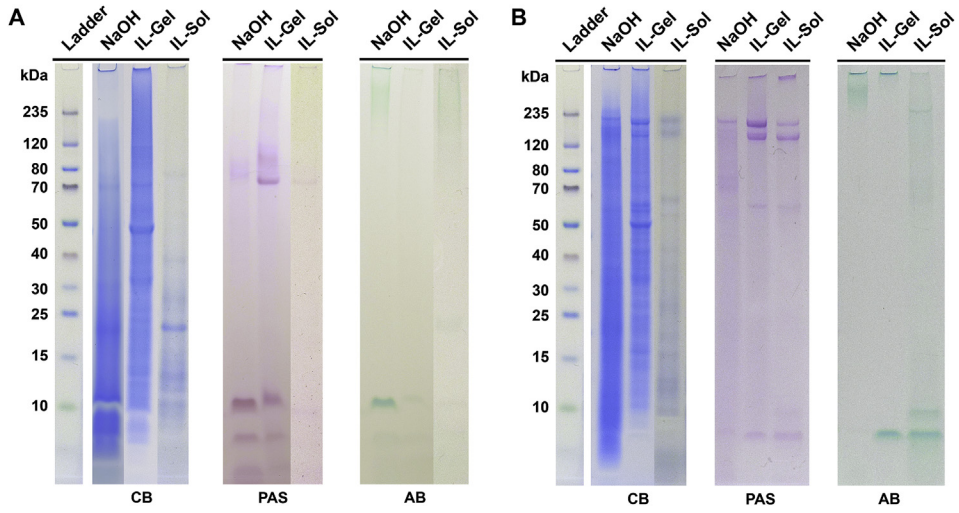

Fig. 8. The different extracted EPS of A) "*Ca.* Brocadia sapporoensis" (NlAmx1) and B) "*Ca.* Brocadia sinica" (NlAmx2) were analysed on a SDS-PAGE gel using different staining's. Coomassie Blue (CB) was applied to stain proteins, Periodic acid Schiff's (PAS) stain for glycans and Alcian Blue (AB) for acidic sugars. (For interpretation of the references to color in this figure legend, the reader is referred to the Web version of this article.)

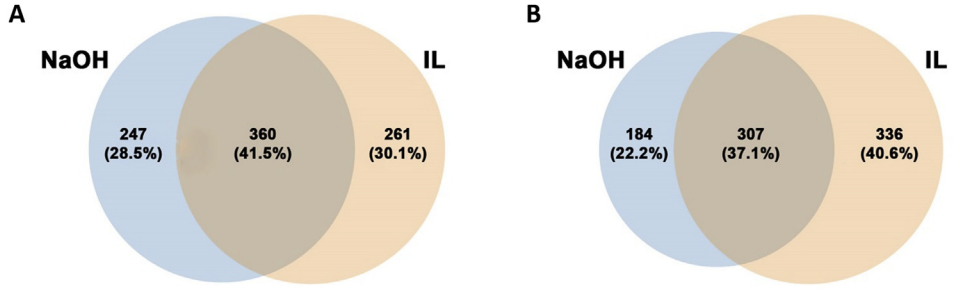

Fig. 9. Venn diagram of the total detected proteins in the NaOH and IL extracts (IL-Gel and IL-Sol taken together), using a "*Ca.* Brocadia" wide database, detected in A) NlAmx1 ("*Ca.* Brocadia sapporoensis") and in B) SgAmx ("*Ca.* Brocadia sinica").

Table 2
Abundant proteins in extracted EPS of NlAmx1 based on the emPAI scores analysis, and their predicted subcellular location and secondary structure (n.d = not detected).

Accession	Annotated function	Species	(%) emPAI			Predicted		
			NaOH	IL-Gel	IL-Sol	Location	β-sheet (%)	α-helix (%)
A0A1V6M2T4	Nitrate oxidoreductase subunit alpha	*Ca.* Brocadia sapporoensis	4.8	5.5	0.1	Periplasm	8	16
A0A1V6LWQ0	Uncharacterized protein	*Ca.* Brocadia sapporoensis	3.5	4.7	3.8	Periplasm	20	5
A0A1V6LWN1	Heme transporter CcmC	*Ca.* Brocadia sapporoensis	3.4	1.6	6.8	Periplasm	4	29
A0A1V6LY92	ATP synthase subunit beta	*Ca.* Brocadia sapporoensis	3.3	3.2	0.4	Cytoplasm	16	34
A0A1V6M2W3	Uncharacterized protein	*Ca.* Brocadia sapporoensis	2.7	1.4	9.4	**Secreted**	3	71
A0A1V6M077	Superoxide dismutase	*Ca.* Brocadia sapporoensis	2.4	1.1	0.4	Cytoplasm	7	58
A0A0C9NKJ8	Nitrate reductase subunit beta	*Ca.* Brocadia sapporoensis	2.2	1.4	n.d.	Periplasm	8	18
A0A1V6LYV6	Serine protease	*Ca.* Brocadia sapporoensis	1.9	1.1	n.d.	Outer Membrane	26	13
A0A1V6LZP8	60 kDa chaperonin	*Ca.* Brocadia sapporoensis	1.8	5.9	5.8	Cytoplasm	12	47
A0A1V6LZQ8	Uncharacterized protein	*Ca.* Brocadia sapporoensis	1.5	1.9	0.6	Periplasm	31	8
A0A1V6LWI7	Uncharacterized protein (Fragment)	*Ca.* Brocadia sapporoensis	1.4	1.6	2.1	**Secreted**	42	0
A0A1V6LXE2	Uncharacterized protein	*Ca.* Brocadia sinica JPN1	1.3	0.7	n.d.	Periplasm	0	29
A0A1V6LYC0	Cysteine synthase A	*Ca.* Brocadia sapporoensis	1.3	1.3	n.d.	Cytoplasm	12	35
A0A1V6M345	Hemerythrin	*Ca.* Brocadia sapporoensis	1.3	n.d	0.3	Cytoplasm	0	20
A0A1V6LZD4	Thioredoxin peroxidase	*Ca.* Brocadia sapporoensis	1.1	n.d.	n.d.	Cytoplasm	25	25
A0A1V6LZX1	ATPase	*Ca.* Brocadia sapporoensis	1.1	n.d.	n.d.	Cytoplasm	9	47
A0A1V6LZI3	60 kDa chaperonin	*Ca.* Brocadia sapporoensis	1.0	2.3	2.3	Cytoplasm	13	47
A0A1V6M3P3	Hydroxylamine oxidoreductase	*Ca.* Brocadia sapporoensis	1.0	0.6	0.5	Periplasm	1	27
A0A1V6M1T3	Glutamate synthase (NADPH), homotetrameric	*Ca.* Brocadia sapporoensis	1.0	0.6	n.d.	Cytoplasm	18	27
A0A1V6LZY1	Probable transaldolase	*Ca.* Brocadia sapporoensis	0.9	0.2	n.d.	Cytoplasm	13	45

(Supplementary Fig. S7).

4. Discussion

4.1. Extracting EPS from anammox granules with two different extraction methods

The EPS are responsible for the stability of biofilms and granular sludge. Knowledge on the composition of the EPS is therefore valuable, because it can aid in development of methods to monitor (e.g. FTIR online measurement), and ultimately control EPS production. Still, it is a poorly characterized material. This is partly due to limitations in extraction methods as well as the analytical methods (Felz et al., 2019; Seviour et al., 2019). Here we analysed EPS of granular sludge of various anammox reactors. Although these four reactors are operated under different conditions, two sets of dominant species were found. In this study, we could correlate the observations of EPS characteristics to the dominant species present, and not to specific reactor conditions. Both the NaOH and IL extractions method could solubilize the anammox granules used in this study, which indicated that at least a part of the structural polymers of the granules was solubilized. In general, both NaOH and IL extractions recovered a range of proteins and glycosylated proteins (with neutral and acidic glycoconjugates). High molecular weight acidic glycoconjugates were more abundant in NaOH than in IL-Gel extracts. Other than that, there were relatively little differences between the NaOH and IL-Gel extracts, that were both recovered after the granular gel matrix was disaggregated. While the IL-Sol fraction, which was recovered when the gel was not solubilized yet, was only a minor fraction and had more differences compared to the two fractions above. This indicates that extraction biases may be reduced when the extraction of EPS is associated with solubilizing the granular matrix.

Looking more in detail to the different fractions, the proteins in both the NaOH and IL-Gel fractions had β-sheets as dominant secondary structure while the proteins in the IL-Sol fraction had α-helixes as the dominant secondary structure. The β-sheet structure was found to be abundant in the granule, indicated by ThT staining. This was also earlier observed for anammox granules (Lotti et al., 2019). In addition the NaOH and IL-Gel fraction contained proteins with a high amount of tryptophan as opposed to IL-Sol (Fig. 7 and Supplementary Fig. S8). Tryptophan-rich EPS was observed in previous studies on EPS of aerobic ammonium oxidizing (AOB) granules (Lin et al., 2018), where it was proposed to play a structural role. Furthermore, phosphate was present in all the fractions, which might relate to the hydroxyapatite accumulation in anammox granules.

Looking at the extraction mechanisms, alkaline treatment can hydrolyse sugars by beta-elimination, and can break disulphide bonds in proteins, which can aid in the disintegration of the EPS matrix (Nielsen and Jahn, 1999). Solubilization by ionic liquids is based on disruption of the hydrogen bonding and its kosmotropic and chaotropic effects. They are also used to stabilize proteins. Wong et al. (2019) showed that the ionic liquid EMIA solubilizes neutral (cellulose) and cationic polysaccharide (chitosan), basic proteins, and to a lesser extend acidic proteins. It does not extract acidic polysaccharides (alginate) as opposed to NaOH, in which acidic polysaccharides are usually more soluble (Wendler et al., 2010). Consistent with these observations, in this study NaOH extracted more acidic glycans from the anammox granules than IL. The fact that the gel matrix was still present after IL treatment, and could only be completely solubilized after addition of the solvent (dimethylacetamide), could indicate a structural role of acidic glycans in the EPS matrix.

Concerning EPS extraction, the choice of the extraction method is dependent on the type of biofilm and on the components that are targeted. To study the structural EPS, it is very important to solubilize the biofilm first. When the composition of the biofilm is unknown, it is suggested to perform a screening of extraction methods to see which one can dissolve the matrix of the biofilm. In the current case, both extraction methods satisfy the requirement of disaggregating the granular structure. The choice is then dependent on the targeted components and follow-up analyses. When anionic components are the target of interest, NaOH is likely more suitable than the ionic liquid EMIA. (Other ionic liquids than EMIA could be more effective for solubilization of acidic glycans.) Since ionic liquids are also used to stabilize proteins, if tertiary structures need to be preserved for analysis, the IL treatment can have advantages over NaOH treatment, which is more prone to cause some hydrolysis of proteins and sugars, and deacetylation of sugars. Here both methods have shown useful to solubilize and characterize the EPS of anammox granular sludge.

Considering the observed damage to the cells during EPS extraction, both methods are likely to cause significant damage. It is worth pointing out that in order to solubilize the structural part of the biofilm, cell damage might be unavoidable during EPS extraction, especially when the granules have compact and strong structures (cell lysis will be further discussed in the next section).

4.2. In search of structural extracellular proteins

Besides the characterization of the structural features and functional groups, MS was applied in order to identify the extracted proteins. Looking at the list of the most abundant identified proteins, it contains intracellular proteins and uncharacterized proteins. Remarkably, various metabolic enzymes, chaperones and elongation factor Tu have been reported in literature as moonlighting proteins (Amblee and Jeffery, 2015). A moonlighting protein is a single protein that can have two or more functions (Ebner et al., 2016). They can have different intra- and extracellular roles. Many of the reported moonlighting proteins work on the cell surface as an adhesin and can bind to structural components like fibronectin, laminin, collagen, or to mucin (Amblee and Jeffery, 2015). These kind of moonlighting proteins were also observed in *Clostridium acetobutylicum* (Liu et al., 2018) and *Staphylococcus aureus* (Foulston et al., 2013) biofilms, and were proposed to play a role in biofilm formation.

In this study we cannot differentiate between possible 'moonlighting proteins' or intracellular proteins that were released during the extractions. However, the possibility of intracellular proteins having an extracellular role underlines that it is very difficult to quantify cell lysis during EPS extraction. During the natural development of granular sludge, intracellular proteins, whether through active secretion or as a result of cell death, can end up in the extracellular matrix (Wingender et al., 1999). Hence, they could already be present before the extraction is applied, and could not be distinguished as intracellular or extracellular proteins. Nevertheless, it is highly likely that there are lysis products released with both extraction methods. Therefore, as proposed by Seviour et al. (2019), the extracellular location of the isolated polymers should always be verified. Location of potential targets can be verified with specific stains, antibodies or lectins (as was for done glycoproteins for example, as described in Boleij et al. (2018)).

4.3. Characterizing the uncharacterized proteins

With the MS analysis no match was obtained that directed to obvious structural extracellular proteins. Likely the proteins that belong to the matrix polymers are among the 'uncharacterized proteins'. In order to clarify the potential function of uncharacterized

proteins, online tools can be used to predict structure, subcellular localization and conserved domains (Ijaq et al., 2015). The protein A0A1V6LWI7 was noticed because it was predicted to be secreted, and to have a secondary structure with a high percentage of β-sheets. The protein has a WD40/YVTN repeat domain, which in general forms structures called β-propellers (Chen et al., 2011). These β-propellers can have various amounts of blades. For this protein a 7-bladed β-propeller structure is predicted, which is reported to have significantly high thermostability and/or thermodynamic stability (Pons et al., 2012). Looking to the aligned PDB structures, the structure of the protein A0A1V6LWI7 is related to hydrazine synthase (Kartal and Keltjens, 2016). On the other hand, the structure was also related to a surface layer protein of archaea bacteria, which was proposed to have a role in cell-cell interactions (Jing et al., 2002). The latter would be interesting considering a role in the extracellular matrix. The protein A0A1V6LWI7 is a potential target to be analysed in more detail, regarding the function in granular sludge. Moreover, localization using e.g. antibodies should be performed to verify it is indeed a secreted protein, or an intracellular protein (or perhaps both). In general, confidence scores for the localization of the proteins, using the prediction tool were low (Supplementary Table S7). This could be due to anammox bacteria having a unique cell compartmentalization with intracellular membranes, unique ladderane membrane lipids, and no standard gram-negative or gram-positive cell wall.

The MS analysis might have not detected, or underestimated part of the extracted proteins. This could be due to recalcitrant proteins not entering the SDS-PAGE gel or due to glycosylation protecting the protein against tryptic digestion, resulting in fewer detected peptides. Another issue is that the database is limited, since it consists of proteins that were annotated from a draft genome. For example, the sequence entry matching the previously identified abundant glycoprotein of "*Ca*. Brocadia sapporoensis" (Boleij et al., 2018) is retracted from the database. When matching the sequence of this protein against the MS spectra of the EPS in this study, it does not come up as an abundant protein, while the band on SDS-PAGE was very abundant. To increase the chance to detect structural matrix proteins, the samples preparation needs to be optimised specifically for the more recalcitrant EPS proteins, e.g. by including a deglycosylation step.

4.4. Concept of the anammox extracellular matrix and outlook

Based on what is currently known, we can make a concept of the organization of the extracellular matrix of anammox granules. In this study and also in previous studies (Johansson et al., 2017; Lin et al., 2013), hydroxyapatite is observed as a part of anammox granules. The EPS matrix may contain the proteins that function as a template for hydroxyapatite formation and thereby provide the 'mineral skeleton' within granules. For example, phosphorylated proteins and acidic groups are both reported to be involved in biomineralization (Ehrlich, 2010; Kawasaki and Weiss, 2006). Furthermore, β-sheet rich proteins present on the cell surface forming the glue in between the cells and the matrix, may be S-layer proteins and/or adhesins. To elucidate the extracellular matrix of anammox granules, the individual components need to be analysed in more detail. For example the glycoprotein for "*Ca.* Brocadia sapporoensis" (Boleij et al., 2018) and for "*Ca*. Brocadia sinica" (Wong et al., 2019) were already characterized in more detail.

5. Conclusions

Global proteomics studies have shed huge insight into many biological processes, however their application to assigning major structural extracellular proteins is limited by extraction techniques, protein solubility and digestibility, and poor representation of extracellular proteins in the reference databases. We addressed the issue of extraction and solubility and observed that while using different extraction methods increases the number of proteins detected, nonetheless the main ones were largely common. We observed by microscopy that the matrix is dominated by β-sheet structures, and confirmed that the extracted proteins had predominately β-sheet structures. Hence, we believe that we extracted structural proteins. However, we could not assign any of the proteins identified from the different extracts by MS as being dominant structural proteins, due to the high number of uncharacterized proteins, potential for moonlighting functions among proteins, and the lack of biophysical data regarding the structures of many of these proteins. Nonetheless, the extraction methods described here enable the biochemical (e.g. isolation) and biophysical approaches needed to fill in the blanks in the protein databases regarding extracellular protein identity and structure.

Declaration of competing interest

The authors declare that they have no known competing financial interests or personal relationships that could have appeared to influence the work reported in this paper.

Acknowledgements

This research was funded by the SIAM Gravitation Grant 024.002.002, The Netherlands Organization for Scientific Research and by the Singapore National Research Foundation under its Environment & Water Research Programme and administered by PUB, project number 1301-IRIS-59. The authors thank Paques, Waterschap Hollandse Delta, and Waterstromen for providing the anammox granular sludge. The authors acknowledge Yingyu Law (SCELSE, Singapore) for assembling the phylogenetic tree. Berend Lolkema (UNESCO-IHE, The Netherlands) is acknowledged for helping with EEM, and Marlies Nijemeisland (TU Delft, The Netherlands) for helping with FTIR.

Appendix A. Supplementary data

Supplementary data to this article can be found online at https://doi.org/10.1016/j.watres.2019.114952.

References

Abma, W.R., Schultz, C.E., Mulder, J.W., van der Star, W.R.L., Strous, M., Tokutomi, T., van Loosdrecht, M.C.M., 2007. Full-scale granular sludge Anammox process. Water Sci. Technol. 55, 27. https://doi.org/10.2166/wst.2007.238.

Agrawal, S., Seuntjens, D., Cocker, P. De, Lackner, S., Vlaeminck, S.E., 2018. Success of mainstream partial nitritation/anammox demands integration of engineering, microbiome and modeling insights. Curr. Opin. Biotechnol. 50, 214–221. https://doi.org/10.1016/j.copbio.2018.01.013.

Amblee, V., Jeffery, C.J., 2015. Physical features of intracellular proteins that moonlight on the cell surface. PLoS One 10, 1–16. https://doi.org/10.1371/journal.pone.0130575.

Barth, A., 2007. Infrared spectroscopy of proteins. Biochim. Biophys. Acta Bioenerg. 1767, 1073–1101. https://doi.org/10.1016/j.bbabio.2007.06.004.

Boleij, M., Pabst, M., Neu, T.R., Van Loosdrecht, M.C.M., Lin, Y., 2018. Identification of glycoproteins isolated from extracellular polymeric substances of full-scale anammox granular sludge. Environ. Sci. Technol. 52, 13127–13135. https://doi.org/10.1021/acs.est.8b03180.

Cao, Y., van Loosdrecht, M.C.M., Daigger, G.T., 2017. Mainstream partial nitritation–anammox in municipal wastewater treatment: status, bottlenecks, and further studies. Appl. Microbiol. Biotechnol. 101, 1365–1383. https://doi.org/10.1007/s00253-016-8058-7.

Chen, C.K.M., Chan, N.L., Wang, A.H.J., 2011. The many blades of the β-propeller proteins: conserved but versatile. Trends Biochem. Sci. 36, 553–561. https://doi.org/10.1016/j.tibs.2011.07.004.

Chen, Z., Meng, Y., Sheng, B., Zhou, Z., Jin, C., Meng, F., 2019. Linking exoproteome function and structure to anammox biofilm development. Environ. Sci. Technol. 53, 1490–1500. https://doi.org/10.1021/acs.est.8b04397.

Ciobanu, C.S., Iconaru, S.L., Massuyeau, F., Constantin, L.V., Costescu, A., Predoi, D., 2012. Synthesis, structure, and luminescent properties of europium-doped hydroxyapatite nanocrystalline powders. J. Nanomater. 2012. https://doi.org/10.1155/2012/942801.

Cirpus, I.E.Y., Geerts, W., Hermans, J.H.M., Op den Camp, H.J.M., Strous, M., Kuenen, J.G., Jetten, M.S.M., 2006. Challenging protein purification from anammox bacteria. Int. J. Biol. Macromol. 39, 88–94. https://doi.org/10.1016/j.ijbiomac.2006.02.018.

De Brabandere, L., Canfield, D.E., Dalsgaard, T., Friederich, G.E., Revsbech, N.P., Ulloa, O., Thamdrup, B., 2014. Vertical partitioning of nitrogen-loss processes across the oxic-anoxic interface of an oceanic oxygen minimum zone. Environ. Microbiol. 16, 3041–3054. https://doi.org/10.1111/1462-2920.12255.

de Graaff, M.S., Temmink, H., Zeeman, G., van Loosdrecht, M.C.M., Buisman, C.J.N., 2011. Autotrophic nitrogen removal from black water: calcium addition as a requirement for settleability. Water Res. 45, 63–74. https://doi.org/10.1016/j.watres.2010.08.010.

Dian, B.C., Longarte, A., Mercier, S., Evans, D.A., Wales, D.J., Zwier, T.S., 2002. The infrared and ultraviolet spectra of single conformations of methyl-capped dipeptides: N-acetyl tryptophan amide and N-acetyl tryptophan methyl amide. J. Chem. Phys. 117, 10688–10702. https://doi.org/10.1063/1.1521132.

Ebner, P., Rinker, J., Götz, F., 2016. Excretion of cytoplasmic proteins in Staphylococcus is most likely not due to cell lysis. Curr. Genet. 62, 19–23. https://doi.org/10.1007/s00294-015-0504-z.

Ehrlich, H., 2010. Chitin and collagen as universal and alternative templates in biomineralization. Int. Geol. Rev. 52 (7-8), 661–699. https://doi.org/10.1080/00206811003679521 .

Felz, S., Al-Zuhairy, S., Aarstad, O.A., van Loosdrecht, M.C.M., Lin, Y.M., 2016. Extraction of structural extracellular polymeric substances from aerobic granular sludge. J. Vis. Exp. JoVE. 115.

Felz, S., Vermeulen, P., van Loosdrecht, M.C.M., Lin, Y.M., 2019. Chemical characterization methods for the analysis of structural extracellular polymeric substances (EPS). Water Res. 157, 201–208. https://doi.org/10.1016/j.watres.2019.03.068.

Flemming, H.C., 2011. The perfect slime. Colloids Surfaces B Biointerfaces 86, 251–259. https://doi.org/10.1016/j.colsurfb.2011.04.025.

Foulston, L., Elsholz, A.K.W., DeFrancesco, A.S., Losick, R., 2013. The Extracellular Matrix of Staphylococcus aureus Biofilms Comprises Cytoplasmic Proteins that Associate with the Cell Surface in Response to Decreasing pH 5, 1–9. https://doi.org/10.1128/mBio.01667-14.

Gasteiger, E., Hoogland, C., Gattiker, A., Wilkins, M.R., Appel, R.D., Bairoch, A., 2005. Protein identification and analysis tools on the ExPASy server. In: The Proteomics Protocols Handbook. Springer, pp. 571–607.

Hoekstra, M., Geilvoet, S.P., Hendrickx, T.L.G., van Erp Taalman Kip, C.S., Kleerebezem, R., van Loosdrecht, M.C.M., 2018. Towards mainstream anammox: lessons learned from pilot-scale research at WWTP Dokhaven. Environ. Technol. 40, 1721–1733. https://doi.org/10.1080/09593330.2018.1470204.

Hou, X., Liu, S., Zhang, Z., 2015. Role of extracellular polymeric substance in determining the high aggregation ability of anammox sludge. Water Res. 75, 51–62. https://doi.org/10.1016/j.watres.2015.02.031.

Ijaq, J., Chandrasekharan, M., Poddar, R., Bethi, N., Sundararajan, V.S., 2015. Annotation and curation of uncharacterized proteins- challenges. Front. Genet. 6, 1–7. https://doi.org/10.3389/fgene.2015.00119.

Jing, H., Takagi, J., Liu, J., Lindgren, S., Zhang, R., Joachimiak, A., Wang, J., Springer, T.A., 2002. Archaeal surface layer proteins contain β propeller, PKD, and β helix domains and are related to metazoan cell. Surface Proteins 10, 1453–1464.

Johansson, S., Ruscalleda, M., Colprim, J., 2017. Phosphorus recovery through biologically induced precipitation by partial nitritation-anammox granular biomass. Chem. Eng. J. 327, 881–888. https://doi.org/10.1016/j.cej.2017.06.129.

Johnson, K., Jiang, Y., Kleerebezem, R., Muyzer, G., van Loosdrecht, M.C.M., 2009. Enrichment of a mixed bacterial culture with a high polyhydroxyalkanoate storage capacity. Biomacromolecules 10, 670–676. https://doi.org/10.1021/bm8013796.

Kalvelage, T., Lavik, G., Lam, P., Contreras, S., Arteaga, L., Löscher, C.R., Oschlies, A., Paulmier, A., Stramma, L., Kuypers, M.M.M., 2013. Nitrogen cycling driven by organic matter export in the South Pacific oxygen minimum zone. Nat. Geosci. 6, 228–234. https://doi.org/10.1038/ngeo1739.

Kartal, B., Keltjens, J.T., 2016. Anammox biochemistry: a tale of heme c proteins. Trends Biochem. Sci. 41, 998–1011. https://doi.org/10.1016/j.tibs.2016.08.015.

Kawasaki, K., Weiss, K.M., 2006. Evolutionary genetics of vertebrate tissue mineralization: the origin and evolution of the secretory calcium-binding phosphoprotein family. J. Exp. Zool. B Mol. Dev. Evol. 306, 295–316.

Lackner, S., Gilbert, E.M., Vlaeminck, S.E., Joss, A., Horn, H., van Loosdrecht, M.C.M., 2014. Full-scale partial nitritation/anammox experiences - an application survey. Water Res. 55, 292–303. https://doi.org/10.1016/j.watres.2014.02.032.

Li, C., Tan, X.F., Lim, T.K., Lin, Q., Gong, Z., 2016. Comprehensive and quantitative proteomic analyses of zebrafish plasma reveals conserved protein profiles between genders and between zebrafish and human. Sci. Rep. 6, 24329.

Lin, Y., Reino, C., Carrera, J., Pérez, J., van Loosdrecht, M.C.M., 2018. Glycosylated amyloid-like proteins in the structural extracellular polymers of aerobic granular sludge enriched with ammonium-oxidizing bacteria. Microbiology (N. Y.) 7 (6). https://doi.org/10.1002/mbo3.616.

Lin, Y.M., Lotti, T., Sharma, P.K., van Loosdrecht, M.C.M., 2013. Apatite accumulation enhances the mechanical property of anammox granules. Water Res. 47, 4556–4566. https://doi.org/10.1016/j.watres.2013.04.061.

Liu, D., Yang, Z., Chen, Y., Zhuang, W., Niu, H., Wu, J., Ying, H., 2018. Clostridium acetobutylicum grows vegetatively in a biofilm rich in heteropolysaccharides and cytoplasmic proteins. Biotechnol. Biofuels 11, 315. https://doi.org/10.1186/s13068-018-1316-4.

Lotti, T., Carretti, E., Berti, D., Martina, M.R., Lubello, C., Malpei, F., 2019. Extraction, recovery and characterization of structural extracellular polymeric substances from anammox granular sludge. J. Environ. Manag. 236, 649–656. https://doi.org/10.1016/j.jenvman.2019.01.054.

Lotti, T., Kleerebezem, R., Lubello, C., Van Loosdrecht, M.C.M., 2014. Physiological and kinetic characterization of a suspended cell anammox culture. Water Res. 60, 1–14.

Møller, H.J., Poulsen, J.H., 2009. Staining of glycoproteins/proteoglycans on SDS-Gels. In: The Protein Protocols Handbook. Springer, pp. 773–777.

Mulder, A., 1989. Anoxic Ammonia Oxidation. European Patent Office - EP 0327184 A1.

Nielsen, P.H., Jahn, A., 1999. Extraction of EPS. In: Wingender, J., Neu, T.R., Flemming, H.-C. (Eds.), Microbial Extracellular Polymeric Substances: Characterization, Structure and Function. Springer Berlin Heidelberg, Berlin, Heidelberg, pp. 49–72. https://doi.org/10.1007/978-3-642-60147-7_3.

Peeters, S.H., van Niftrik, L., 2019. Trending topics and open questions in anaerobic ammonium oxidation. Curr. Opin. Chem. Biol. 49, 45–52. https://doi.org/10.1016/j.cbpa.2018.09.022.

Pena-Francesch, A., Demirel, M.C., 2019. Squid-inspired tandem repeat proteins: functional fibers and films. Front. Chem. 7, 1–16. https://doi.org/10.3389/fchem.2019.00069.

Perras, A.K., Daum, B., Ziegler, C., Takahashi, L.K., Ahmed, M., Wanner, G., Klingl, A., Leitinger, G., Kolb-Lenz, D., Gribaldo, S., Auerbach, A., Mora, M., Probst, A.J., Bellack, A., Moissl-Eichinger, C., 2015. S-layers at second glance? Altiarchaeal grappling hooks (hami) resemble archaeal S-layer proteins in structure and sequence. Front. Microbiol. 6. https://doi.org/10.3389/fmicb.2015.00543.

Pons, T., Gómez, R., Chinea, G., Valencia, A., 2012. Beta-propellers: associated functions and their role in human diseases. Curr. Med. Chem. 10, 505–524. https://doi.org/10.2174/0929867033368204.

Pronk, M., Neu, T.R., van Loosdrecht, M.C.M., Lin, Y.M., 2017. The acid soluble extracellular polymeric substance of aerobic granular sludge dominated by Defluviicoccus sp. Water Res. 122, 148–158. https://doi.org/10.1016/j.watres.2017.05.068.

Seviour, T., Derlon, N., Dueholm, M.S., Flemming, H.-C., Girbal-Neuhauser, E., Horn, H., Kjelleberg, S., van Loosdrecht, M.C.M., Lotti, T., Malpei, M.,F., Nerenberg, R., Neu, T.R., Paul, E., Yu, H., Lin, Y., 2019. Extracellular polymeric substances of biofilms: suffering from an identity crisis. Water Res. 151, 1–7. https://doi.org/10.1016/j.watres.2018.11.020.

Seviour, T., Weerachanchai, P., Hinks, J., Roizman, D., Rice, S.a., Bai, L., Lee, J., Kjelleberg, S., 2015. Solvent optimization for bacterial extracellular matrices: a solution for the insoluble. RSC Adv. 5, 7469–7478. https://doi.org/10.1039/C4RA10930A.

van der Star, W.R.L., Abma, W.R., Blommers, D., Mulder, J.-W., Tokutomi, T., Strous, M., Picioreanu, C., van Loosdrecht, M.C.M., 2007. Startup of reactors for anoxic ammonium oxidation: experiences from the first full-scale anammox reactor in Rotterdam. Water Res. 41, 4149–4163. https://doi.org/10.1016/j.watres.2007.03.044.

Van Teeseling, M.C.F., Neumann, S., Van Niftrik, L., 2013. The anammoxosome organelle is crucial for the energy metabolism of anaerobic ammonium oxidizing bacteria. J. Mol. Microbiol. Biotechnol. 23, 104–117.

Vlaeminck, S.E., Terada, A., Smets, B.F., der Linden, D., Boon, N., Verstraete, W., Carballa, M., 2009. Nitrogen removal from digested black water by one-stage partial nitritation and anammox. Environ. Sci. Technol. 43, 5035–5041. https://doi.org/10.1021/es803284y.

Wendler, F., Meister, F.F., Wawro, D., Wesolowska, E., Saake, B., Puls, J.J., Moigne, N. Le, Navard, P., Wendler, F., Meister, F.F., Wawro, D., Wesolowska, E., Ciechanska, D., Wendler, F., Meister, F.F., Wawro, D., Puls, J.J., Moigne, N. Le, Navard, P., Saake, B., Puls, J.J., Le Moigne, N., Navard, P., 2010. Polysaccharide blend fibres formed from NaOH, N-methylmorpholine-N-oxide and 1-ethyl-3-methylimidazolium acetate. Fibres Text. East Eur vol. 18, 21.

Wingender, J., Neu, T.R., Flemming, H.-C., 1999. What are bacterial extracellular polymeric substances? In: Wingender, J., Neu, T.R., Flemming, H.-C. (Eds.), Microbial Extracellular Polymeric Substances: Characterization, Structure and Function. Springer Berlin Heidelberg, Berlin, Heidelberg, pp. 1–19. https://doi.org/10.1007/978-3-642-60147-7_1.

Wong, L.L., Natarajan, G., Boleij, M., Thi, S.S., Winnerdy, F.R., Mugunthan, S., Lu, Y., Lee, J.-M., Lin, Y., Loosdrecht, M. van, Law, Y., Kjelleberg, S., Seviour, T.W., 2019. Isolation of a putative S-layer protein from anammox biofilm extracellular matrix using ionic liquid extraction. bioRxiv 705566. https://doi.org/10.1101/705566.

Yachdav, G., Kloppmann, E., Kajan, L., Hecht, M., Goldberg, T., Hamp, T., Hönigschmid, P., Schafferhans, A., Roos, M., Bernhofer, M., Richter, L., Ashkenazy, H., Punta, M., Schlessinger, A., Bromberg, Y., Schneider, R., Vriend, G., Sander, C., Ben-Tal, N., Rost, B., 2014. PredictProtein - an open resource for online prediction of protein structural and functional features. Nucleic Acids Res. 42, 337–343. https://doi.org/10.1093/nar/gku366.

Yang, X.R., Li, H., Nie, S.A., Su, J.Q., Weng, B. Sen, Zhu, G.B., Yao, H.Y., Gilbert, J.A., Zhu, Y.G., 2015. Potential contribution of anammox to nitrogen loss from paddy soils in southern China. Appl. Environ. Microbiol. 81, 938–947. https://doi.org/10.1128/AEM.02664-14.